EXPERIMENTAL INVESTIGATION OF THE STRESS-STRAIN STATE PRODUCED IN LOESS SOILS OF VARYING MOISTURE CONTENT BY AN EXPLOSION

V. V. Mel'nikov and G. V. Rykov

Zhurnal Prikladnoi Mekhaniki i Tekhnicheskoi Fiziki, No. 1, pp. 148-152, 1966

Reference [1] reported the results of an experimental investigation of spherical blast waves in loess soils of undisturbed structure and natural moisture content. Below we present the results of analogous investigations of the same soils but with different moisture contents (w = 19-21% and 22-25% with δ = 1.34-1.38 g/cm^3, where w is the mass moisture content, and δ is the weight by volume of the soil skeleton). The experiments were based on a method previously described in [2, 3]. The principal normal stresses, radial and tangential, were measured as in [1-3] with the help of high-frequency membrane strain gauges whose signals were recorded on MPO-2 and N-102 oscillographs. The particle velocities were measured by probes consisting of a solenoid in a metal housing with a cylindrical permanent magnet freely moving inside the solenoid. The variable moisture content of soils with undisturbed structure was obtained by first wetting them on specially prepared tables, thus ensuring that the experiments were conducted under uniform moistening conditions. Some of the experiments were performed on soils with a disturbed structure (δ = 1.30-1.34 g/cm^3 at w = 19-21%). The experimental data were reduced by the method of least squares.

1. Figure 1 gives the stress and particle velocity oscillograms corresponding to the explosion of a charge of weight C = 0.2 kg in loess soil of undisturbed structure with w = 19-21% at a depth $h/r_3 = 20$, where $r_3 = 0.054\,C^{1/3}$ is the charge radius, and h is the distance from the soil surface to the center of the charge.

The first and second traces of the first oscillogram (reckoning from top to bottom) correspond to the radial stress σ_r and the tangential stress σ_α at a distance R = 10; the third and fourth traces correspond to σ_r and σ_α at a distance R = 15. Here $R = r/r_3$ is the dimensionless distance from the center of the charge. The fifth trace fixes the explosion.

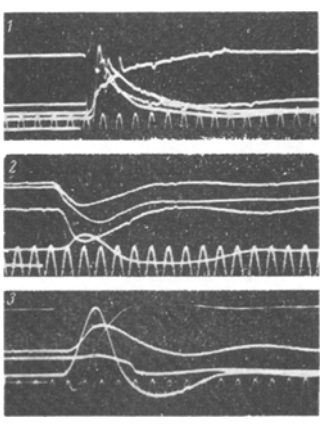

Fig. 1

The first and second traces of the second oscillogram correspond to σ_r and σ_α at a distance R = 20; the third and fourth traces to σ_r and σ_α at a distance R = 30. In the third oscillogram the first, second and third traces correspond to the velocity of the soil particles at distances R = 10, 20 and 30. The period of oscillation of the time mark is 0.002 sec.

It is clear from the oscillograms that in loess soils with increased moisture content shock waves occur, as in loess soils of natural moisture content (w = 13-14%), only at fairly short distances up to R = 10-15 at stresses σ_r > 15-20 kg/cm^2. At greater distances at σ_r < < 15-20 kg/cm^2 the blast waves take the form of compression waves with a gradual increase in stress to the maximum value. A similar picture is observed in loess soils with a disturbed structure.

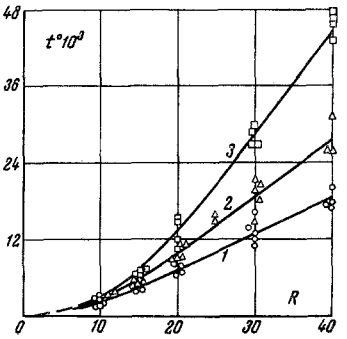

Fig. 2

An analysis of the experimental data showed that, on the whole, the laws of attenuation of blast waves in loess soils of different moisture content are similar [1-3] and may be described by the same empirical formulas. In particular, for the maximum stresses and specific impulses we have

$$\sigma_r^m = K_1 \cdot R^{-\mu_1} \text{ kg/cm}^2, \qquad \sigma_\alpha^m = K_1' \cdot R^{-\mu_1} \text{ kg/cm}^2, \tag{1.1}$$

$$I_r^\circ = K_2 \cdot R^{-\mu_2} \text{ kg} \cdot \text{sec}^2/\text{cm}^2 \cdot \text{kg}^{1/3}, \qquad I_\alpha^\circ = K_2' \cdot R^{-\mu_2} \text{ kg} \cdot \text{sec}^2/\text{cm}^2 \cdot \text{kg}^{1/3}, \tag{1.2}$$

where σ_r^m and σ_α^m are respectively the maximum radial and tangential stresses, and I_r° and I_α° are respectively the specific impulses of the radial and tangential stresses.

Here and henceforth the superscript "°" denotes that the quantity has been divided by the scale of the phenomenon, i.e., by $C^{1/3}$, where C is the weight of the charge in kg.

We present values of the experimental coefficients K_1, K_1', μ_1, K_2, K_2' and μ_2:

K_1	K_1'	μ_1	K_2	K_2'	μ_2	ξ
$9.0\cdot10^3$	$3.6\cdot10^3$	2.42	7.40	2.96	1.61	0.40
$10.2\cdot10^3$	$4.6\cdot10^3$	2.43	4.26	1.92	1.35	0.45
$7.1\cdot10^3$	$3.5\cdot10^3$	2.39	2.88	1.44	1.15	0.50.

Here and henceforth in the values of the coefficients the first row corresponds to undisturbed loess soil with w = 19-21%, the second row to w = 22-25%, and the third row to disturbed loess soil with ρ = = 1.30-1.34 g/cm^3 and w = 19-21%.

A comparison of the data with the analogous data of [1] shows that the maximum radial stresses change only slightly with increase in moisture content; disturbing the structure leads to a decrease in stress at corresponding distances as compared with soil with undisturbed structure and the same moisture content. In this case the value of the lateral pressure coefficient $\xi = \sigma_\alpha^m / \sigma_r^m$ increases with increase in moisture content and with disturbance of the soil structure. The impulses I_r° and I_α° also increase with increase in moisture content and with disturbance of the soil structure.

Figure 2 gives hodographs of the shock fronts and maximum stresses. The circles represent the experimental data referred to a soil with undisturbed structure and w = 19-21%; the triangles the data for w = 22-25%. The squares represent the experimental

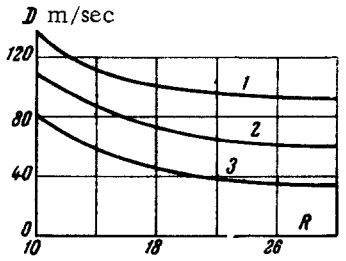

Fig. 3

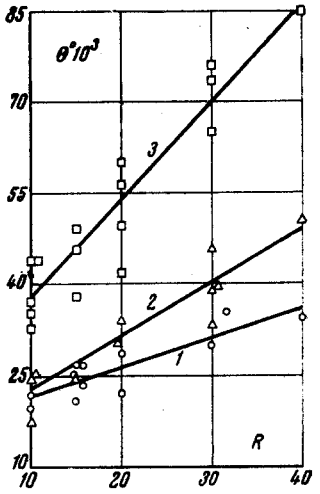

Fig. 4

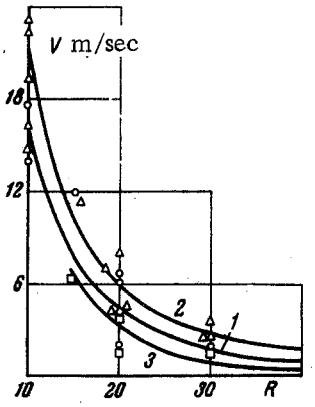

Fig. 5

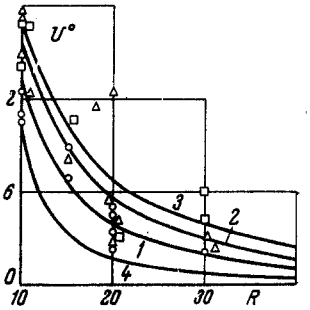

Fig. 6

data for a soil with disturbed structure with w = 19-21% (the same notation is retained in subsequent graphs). Each of these curves is approximated, as in [1], by two empirical formulas,

$$t^\circ = K_3 \cdot (R^{\mu_3} - 1) \cdot 10^{-3} \text{ sec/kg}^{1/3}, \quad 10 \leqslant R \leqslant 25, \qquad (1.3)$$

$$t^\circ = (a_1 + \eta_1 R) \cdot 10^{-3} \text{ sec/kg}^{1/3}, \quad 25 \leqslant R \leqslant 40, \qquad (1.4)$$

where t° is the time of arrival of the wave front (or maximum stress) at a given point in space; K_3, μ_3, a_1 and η_1 are experimental coefficients

K_3	μ_3	a_1	η_1	a_0, m/sec	a_2	η_2
0.1150	1.40	—4.25	0.585	360	16.50	0.500
0.0665	1.66	—9.40	0.930	372	13.55	0.865
0.0371	1.96	—19.85	1.605	126	22.00	1.600

Differentiating (1.3) and (1.4) with respect to t, we get, as in [1, 3], formulas for determining the velocity of propagation of the shock wave (or maximum stresses)

$$D = \frac{54}{\mu_3 K_3 R^{\mu_3 - 1}}, \quad \text{m/sec} \quad 10 \leqslant R \leqslant 25, \qquad (1.5)$$

$$D = \frac{54}{\eta_1}, \quad \text{m/sec} \quad R \geqslant 25. \qquad (1.6)$$

The velocity graphs corresponding to (1.5), (1.6) are presented in Fig. 3. As follows from Fig. 3 and [1], the velocities of propagation of the shock front and maximum stresses decrease with increase in moisture content from w = 12-13% to w = 22-25% by a factor of 1.5-2.

When the structure is disburbed (curves 1, 3 of Fig. 3) the velocity of propagation of the maximum stresses also decreases by a factor of two. The velocity of the elastic waves a_0 increases only slightly with increase in moisture content—from a_0 = 350 m/sec for w = 12-13% [1] to a_0 = 372 m/sec for w = 22-25%.

Figure 4 gives the experimental data on the variation with distance of the time of action of the wave θ_1; these are well approximated by the linear law [3]

$$\theta^\circ = (a_2 + \eta_2 R) 10^{-3} \text{ sec/kg}^{1/3}. \qquad (1.7)$$

Values of a_2 and η_2 were presented above. As may be seen from Fig. 4, with increase in moisture content, and especially with disturbance of structure, the time of action increases.

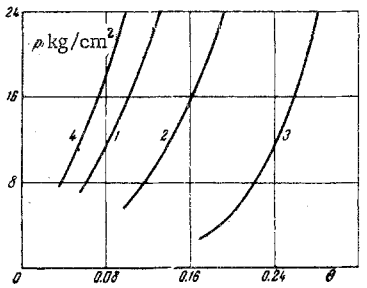

Fig. 7

Figures 5 and 6 give experimental data on the variation with distance from the center of the charge of the maximum particle velocities (Fig. 5) and maximum displacements of the soil (Fig. 6). The corresponding empirical formulas are

$$V_m = K_4 R^{-\mu_4} \text{ m/sec}, \qquad U_m^\circ = K_5 \cdot R^{-\mu_5} \text{ cm/kg}^{1/3} \qquad (1.8)$$

Here K_4, μ_4, K_5 and μ_5 are experimental coefficients

K_4	μ_4	K_5	μ_5	k	b
$1.46 \cdot 10^3$	1.94	6.82	1.72	1.41	1.20
$1.58 \cdot 10^3$	1.88	6.55	1.60	1.23	0.50
$1.05 \cdot 10^3$	2.70	3.64	1.34	1.06	0.40

For comparison, Fig. 6 gives the displacement curve 4 for soil with w = 12-13% [1]. An analysis of the data for loess soils with different moisture contents shows that at similar distances with increase from w = 12-13% to w = 22-25% the displacements increase by 2-4 times.

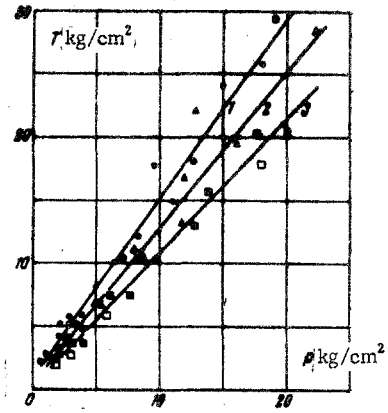

Fig. 8

2. The data obtained permit a number of conclusions concerning the compressibility and plastic properties of the soils investigated [1-3].

Using the laws of conservation of mass and momentum at the shock front, we get, as in [3], the diagram of volume compression under load,

$$p_\sigma = m \cdot \varepsilon_\sigma^\nu, \quad m = \frac{1 + 2\xi_0}{3} \cdot K_1 \cdot \varepsilon_1^{-\mu_1/n}, \quad \varepsilon_1 = \frac{K_1}{\rho_0} \left(\frac{\mu_3 \cdot K_3}{54} \right)^2,$$

$$\rho_0 = (1 + 0.01\, w) \cdot \frac{\delta}{g}; \quad n = \mu_1 - 2(\mu_3 - 1), \quad \nu = \frac{\mu_1}{\eta}; \qquad (2.1)$$

Here ρ_0 is the initial density of the soil.

Figure 7 gives graphs constructed from (2.1) for all the cases considered. Clearly, the change in moisture content has a substantial effect on the compressibility of loess soils. Thus, as w varies from 13-14% (curve 4) to 22-25% (curve 3) the strains increase by 2-3 times (at p = 8-24 kg/cm^2). Obviously, in this case there is manifested to a very high degree such distinctive properties of loess soils as their capacity for very considerable settlement and subsidence. Under short-time dynamic loads it is not possible to follow the development of the settlement, which is so typical of loess soils under constant static loads, but usually occurs over much longer periods of time. Clearly, in examining the behavior of loess soils under dynamic loads one should not attempt to isolate settlement as an independent characteristic, but consider only the over-all deformation capacity of the soil.

An analysis of the measured radial and tangential stresses revealed that, as shown previously [1-3], the yield condition for loess soils of different moisture content has the form

$$I_2 = \frac{1}{6} F^2(p) = \frac{1}{6} (kp + b)^2, \qquad (2.2)$$

where k and b are experimental coefficients characterizing the internal friction and cohesion in the soil, $I_2 = S_{ij}S_{ij}/2$; $S_{ij} = \sigma_{ij} + p\delta_{ij}$ $(i, j = 1, 2, 3)$, σ_{ij} are the stress tensor components, and $p = -\frac{1}{3}\sigma_{ii}$ is the mean hydrostatic pressure.

Figure 8 gives the experimental data on the relation between $T = \sqrt{6I_2}$ and p for the cases considered. The blacked-in symbols relate to the experimental points corresponding to loading, the open symbols to unloading.

An analysis of Fig. 8 shows that with increase in moisture content the coefficients of internal friction k and cohesion b decrease. Disturbance of the structure leads to an even sharper decrease in these coefficients.

It is important to note that the yield condition for loading and unloading is the same.

The authors are indebted to S. S. Grigoryan for assisting with the experiments and discussing the results, and to G. M. Lyakhov and S. D. Mizyakin for helping with the organization and carrying out of the experiments.

REFERENCES

1. S. S. Grigoryan, G. M. Lyakhov, V. V. Mel'nikov, and G. V. Rykov, "Blast waves in loess soils," PMTF, no. 4, 1963.

2. V. D. Alekseenko, S. S. Grigoryan, L. I. Koshelev, A. F. Novgorodov, and G. V. Rykov, "Measurement of stress waves in soft soils," PMTF, no. 2, 1963.

3. G. V. Rykov, "Experimental investigation of the stress field produced by an explosion in sandy soil," PMTF, no. 1, 1964.

14 June 1965 Moscow